Hierarchical CuO@CuS core/shell Nanowires for Supercapacitor Electrode Materials

Yasar Ozkan Yesilbag
Department of Physics
Erzincan Binali Yıldırım University
Erzincan, Turkey
oyesilbag@erzincan.edu.tr

Fatma Nur Tuzluca
Department of Physics
Erzincan Binali Yıldırım University
Erzincan, Turkey
ftuzluca@erzincan.edu.tr

Mehmet Ertugrul
Department of Electrical and Electronics Engineering
Ataturk University
Erzurum, Turkey
ertugrul@atauni.edu.tr

***Abstract*—Hierarchical CuO@CuS core/shell nanowires (NWs) array is directly synthesized on Cu foam using thermal oxidation and hydrothermal method respectively. The structure, morphology and electrochemical performance of CuO@CuS core/shell NWs arrays are systematically characterized by X-Ray Diffraction Spectroscopy (XRD), Field Emission Scanning Electron Microscopy (FESEM), Energy Dispersion X-Ray Spectroscopy (EDS), Cyclic Voltammetry (CV) and Galvanostatic Charge/Discharge (GCD). This electrode structure demonstrates good electrochemical performance with a maximum areal capacitance of 343 mF cm^{-2} at 2 mA cm^{-2}.**

Keywords—CuO@CuS core/shell nanowires, supercapacitor, thermal oxidation.

I. INTRODUCTION

In recent years, supercapacitors are of particular interest due to their high power density, fast charge/discharge rate and long cycle life [1]–[3]. Supercapacitors are divided into two types depending on the charge storage mechanisms - electrical double layer capacitors (EDLCs) and pseudocapacitors [3]. EDLCs store charge electrostatically at electrode/electrolyte interface as charge separation. There is no charge transfer between electrode and electrolyte. Pseudocapacitors store by charge transfer between electrode and electrolyte. The charge is transferred at the surface or in the bulk near the surface through adsorption, redox reaction and intercalation of ions [4]. Transition metal oxides and hydroxides are being extensively investigated for use in high performance supercapacitors due to their low cost and low toxicity [5]. Among these metal oxides, CuO has attractive features like low cost, abundant resources, non-toxicity, and easy preparation in diverse shapes of nano-sized dimension, such as nanowires, nanospheres, nanoflowers, nanorods, and nanotubes [6]. It has been extensively studied as a p-type metal-oxide semiconductor [7]. Having direct bandgap of about 1.2 eV and exhibits many excellent physical and chemical properties [8], [9]. CuO have been widely used in many areas such as in anode electrodes for batteries and supercapacitors [10], photovoltaic cells [11], field emission nanodevices [12], and gas sensors [13]. Different approaches have been employed to synthesize 1-D CuO nanostructures such as the hydrothermal method, the thermal decomposition method, and the templating sol-gel method [6].

Recently, different transition metal sulfides such as CoS [14], NiS [15], ZnS [16], and CuS [17], [18] have been investigated as pseudocapacitive electrode materials due to their high electrochemical performance. Among these transition metal sulfides, CuS is used as electrode material because of low cost, abundance, different morphology in nanoscale and metal-like electronic conductivity (10^{-3} S/cm). In this work, firstly large-scale vertically aligned single crystalline CuO NWs have been synthesized on copper foam at 500°C for 4 h via thermal oxidation method. After then CuS were synthesized on CuO NWs via hydrothermal method to enhance the active sites and the electronic conductivity.

II. MATERIAL AND METHOD

First of all, large-scale vertically aligned single crystalline CuO NWs were synthesized on Cu foam thermal oxidation method. To remove the oxide layer on the surface the Cu foam, it was cleaned in ultrasonic cleaner for 1 M HCl (50 ml) de-ionized water, absolute ethanol 15 min respectively. The solution of 10 mmol urea (CH_4N_2O) and 10 mmol ammonium fluoride (NH_4F) with Cu foam was transferred into a teflon-lined stainless steel autoclave and heated at 120°C for 12 h. The Cu foam was then annealed in air at 500°C in the tube furnace and kept for 4 h to obtain CuO NWs. To obtain CuO@CuS core/shell NWs structure, the sample was then placed in an autoclave with 2 mmol of thioacetamide (C_2H_5NS) solution dissolved in 35 ml of de-ionized water. The autoclave was heated at 90°C for 1 h. After this process, the autoclave cooled down to room temperature and the sample was dried at 80°C for 2 h.

The crystal structures and morphologies of the CuO@CuS core/shell NWs were determined by using X-Ray Diffraction (PANalytical Empyrean, Cu-Kα, λ=1.54060 Å), Field Emission Scanning Electron Microscopy (FEI Quanta 450 FEG) and Energy Dispersion X-Ray Spectroscopy (EDAX, AMETEK Materials Analysis Division). The electrochemical performance were determined by Cyclic Voltammetry and Galvanostatic Charge Discharge analyses using a Gamry Reference 1010E potentiostat instrument.

The electrochemical measurements were performed using 2 M KOH aqueous electrolyte solution. Platinum foil (1 × 1 cm^2 in area) and the Ag/AgCl were used as the counter and reference electrodes, respectively. The CuO@CuS electrode (1 × 1 cm^2) were immersed in electrolyte and were used directly as a working electrode. The electrochemical measurements were performed in a three-electrode electrochemical cell at room temperature. The areal capacitance (C) was calculated by equation (1):

$$C = \frac{Ixt}{AxV} \qquad (1)$$

where ***I*** is the constant discharge current, ***t*** is the discharge time, ***V*** is the potential window and ***A*** is the electrode area.

III. RESULTS AND DISCUSSION

The XRD diffraction patterns of the sample taken over a 20° to 80° (2θ) range are given in Fig. 1. The XRD peaks can be indexed as monoclinic structured CuO (JCPDS card No. 80-1917), cubic structured cuprous oxide (Cu2O) (JCPDS card No. 78-2076), and fcc Cu metal from the substrate (JCPDS card No. 85-1326). After sulfonation reaction, some diffraction peaks indexed to hexagonal-phase CuS (JCPDS card No. 06-0464). The sharp and intense peaks in the XRD patterns of CuO@CuS core/shell NWs arrays indicate their good crystallinity.

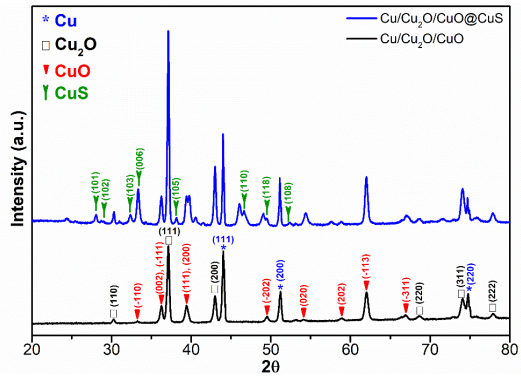


Fig. 1. XRD patterns of CuO and CuO@CuS core/shell NWs.

Fig. 2 shows the FESEM images and EDS analyzes of the morphology of CuO NWs arrays. As seen in figure, CuO NWs have grown onto the Cu foam surface densely and uniformly. The purity and composition of the CuO NWs were further confirmed by EDS analysis. EDS spectrum revealing the existence of Cu and O elements in the sample. According to EDS analysis, the atomic contents of Cu and O are 53.84% and 46.16%, which is nearly in agreement with the 1:1 stoichiometric ratio of CuO NWs, respectively. After sulfur treatment, FESEM images and EDS analyzes of CuO@CuS core/shell NWs arrays are given in Fig. 3. It can been clearly seen that, CuS structure is formed on the surface of CuO NWs. Further analysis with EDAX measurement, only strong peaks for Cu, S and O are found in the spectrum. The atomic ratio of Cu, S and O is 50.57%, 42.50% and 6.92%.

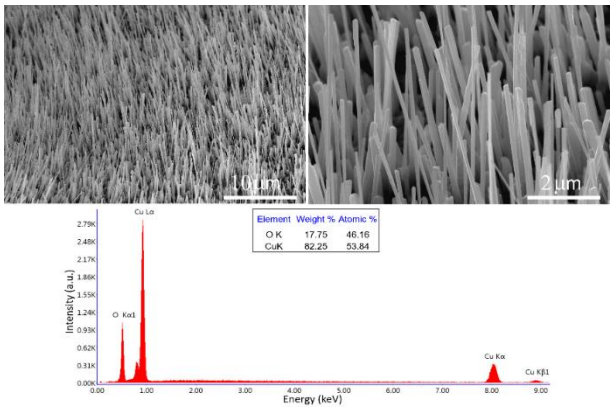


Fig. 2. Low and high magnification FESEM images and EDS analyzes of CuO NWs.

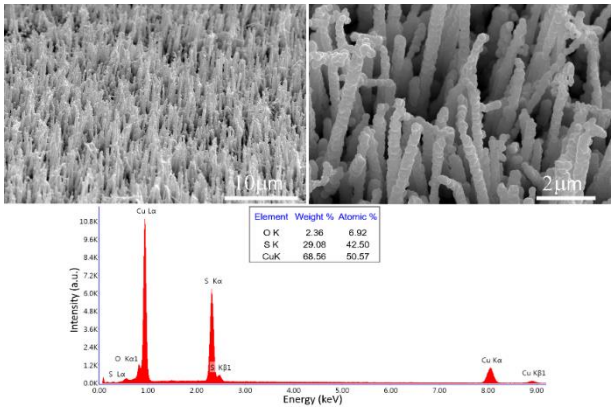


Fig. 3. Low and high magnification FESEM images and EDS analyzes of CuO@CuS core/shell NWs.

Electrochemical properties of CuO@CuS electrode in 2 M KOH aqueous electrolyte are shown in Fig. 4. In Fig. 4a, the typical CV curves of the CuO@CuS electrode measured at various scan rates ranging from 5 to 100 mV s^{-1}. It can be seen that the CV curves of the CuO@CuS electrode have two redox peaks, which reveal that pseudocapacitive characteristics of these electrode. In order to evaluate the areal capacitance, GCD measurements were performed. The GCD curves of the CuO@CuS electrode in the voltage range of −0.5 to 0.2 V at various current densities of 2 to 6 mA cm^{-2} are illustrated in Fig. 4b. The nonlinear behavior of the GCD curves confirms that the charge storage in the CuO@CuS electrode mainly originates from pseudocapacitance mechanism. The areal capacitance values of the CuO@CuS core/shell NWs arrays were 343, 257, 171, 107 and 68 mF cm^{-2} at current densities of 2, 3, 4, 5 and 6 mA cm^{-2}, respectively in Fig. 4c.

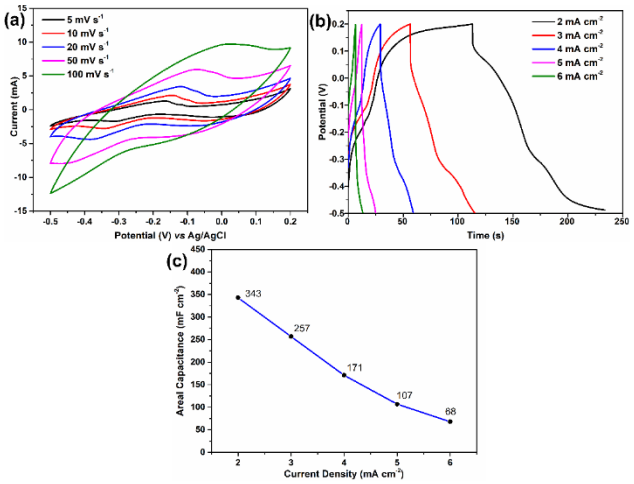


Fig. 4. (a) The CV curves at different scan rates, (b) the GCD curves at different current densities, (c) the areal capacitance vs. different current density.

IV. CONCLUSION

In conclusion, CuO@CuS core/shell NWs were synthesized on Cu foam by thermal oxidation and hydrothermal method respectively. According to GCD measurements at 2 mA cm^{-2} current density, areal capacitance were obtained 343 mF cm^{-2} for CuO@CuS core/shell NWs. This study also gives different point of view

into the design of metal oxide/sulfide heterostructure electrodes used in a various range of applications.

ACKNOWLEDGEMENT

This research is partially supported by Erzincan Binali Yıldırım University Scientific Research Project Unit (Project number: FBA-2017-468).

REFERENCES

[1] G. Wang, L. Zhang, and J. Zhang, "A review of electrode materials for electrochemical supercapacitors," *Chem. Soc. Rev.*, vol. 41, pp. 797–828, 2012.

[2] Y. Zhang, L. Li, H. Su, W. Huang, and X. Dong, "Binary metal oxide: advanced energy storage materials in supercapacitors," *J. Mater. Chem. A*, vol. 3, no. 1, pp. 43–59, 2015.

[3] F. Beguin, V. Presser, A. Balducci, and E. Frackowiak, "Carbons and electrolytes for advanced supercapacitors," *Adv. Mater.*, vol. 26, no. 14, pp. 2219–2251, 2014.

[4] V. Augustyn, P. Simon, and B. Dunn, "Pseudocapacitive oxide materials for high-rate electrochemical energy storage," *Energy Environ. Sci.*, vol. 7, no. 5, p. 1597, 2014.

[5] F. Shi, L. Li, X. Wang, C. Gu, and J. Tu, "Metal oxide/hydroxide-based materials for supercapacitors," *RSC Adv.*, vol. 4, no. 79, pp. 41910–41921, 2014.

[6] Q. Zhang *et al.*, "CuO nanostructures: Synthesis, characterization, growth mechanisms, fundamental properties, and applications," *Prog. Mater. Sci.*, 2014.

[7] J. Huang, Y. Zhu, X. Yang, W. Chen, Y. Zhou, and C. Li, "Flexible 3D porous CuO nanowire arrays for enzymeless glucose sensing: In situ engineered versus ex situ piled," *Nanoscale*, 2015.

[8] D. Li, J. Hu, R. Wu, and J. G. Lu, "Conductometric chemical sensor based on individual CuO nanowires," *Nanotechnology*, vol. 21, no. 48, 2010.

[9] M. Vila, C. Díaz-Guerra, and J. Piqueras, "Optical and magnetic properties of CuO nanowires grown by thermal oxidation," *J. Phys. D. Appl. Phys.*, 2010.

[10] Q. Zhang, J. Wang, D. Xu, Z. Wang, X. Li, and K. Zhang, "Facile large-scale synthesis of vertically aligned CuO nanowires on nickel foam: Growth mechanism and remarkable electrochemical performance," *J. Mater. Chem. A*, 2014.

[11] B. G. Ganga, S. M. Seetharaman, P. C. R. Varma, M. A. G. Namboothiry, and P. N. Santhosh, "Photovoltaic properties of low temperature solution processed earth abundant CuO nanocrystal-based hybrid solar cells," *Phys. status solidi*, vol. 214, no. 1, p. 1600671, Jan. 2017.

[12] G. Kaur, K. Saini, A. K. Tripathi, V. Jain, D. Deva, and I. Lahiri, "Room temperature growth and field emission characteristics of CuO nanostructures," *Vacuum*, 2017.

[13] M. Yin, F. Wang, H. Fan, L. Xu, and S. Liu, "Heterojunction CuO@ZnO microcubes for superior p-type gas sensor application," *J. Alloys Compd.*, 2016.

[14] H. Hu, B. Y. Guan, and X. W. (David) Lou, "Construction of Complex CoS Hollow Structures with Enhanced Electrochemical Properties for Hybrid Supercapacitors," *Chem*, 2016.

[15] A. Wang *et al.*, "Controlled synthesis of nickel sulfide/graphene oxide nanocomposite for high-performance supercapacitor," *Appl. Surf. Sci.*, 2013.

[16] N. S. Arul, L. S. Cavalcante, and J. In Han, "Facile synthesis of ZnS/MnS nanocomposites for supercapacitor applications," *J. Solid State Electrochem.*, 2018.

[17] H. Heydari, S. E. Moosavifard, S. Elyasi, and M. Shahraki, "Nanoporous CuS nano-hollow spheres as advanced material for high-performance supercapacitors," *Appl. Surf. Sci.*, 2017.

[18] W. Xu *et al.*, "Synthesis and properties of morphology controllable copper sulphide nanosheets for supercapacitor application," *Electrochim. Acta*, 2016.